Textile Research Journal

Original article

Textile Research Journal
0(0) 1–22

DOI: 10.1177/00405175251358497
journals.sagepub.com/home/trj
Sage

Example-based approach for automatic garment pattern generation

Roujia Hong[1], Yarui Zhang[1], Qi Zhang[1], Diqing Qian[2,3], Yao Jin[1,2], Huaxiong Zhang[1] and Lili He[1,2]

Abstract

This paper proposes an example-based method for automated garment pattern generation, addressing challenges in craftsmanship standardization and geometric fidelity in existing 2D pattern techniques. This approach integrates graph neural network (GNN)-based garment panel segmentation with manufacturing-constrained flat pattern modeling to establish a seamless bridge between digital fashion design and traditional garment craftsmanship. More specifically, a sparse graph transformer is employed to efficiently segment 3D garment meshes into individual panels. Leveraging the technique of virtual node sparsification, this method remarkably reduces the computational complexity, enabling a more efficient segmentation process. To ensure its practical viability in industrial applications, the methodology incorporates two critical types of manufacturing constraints. Symmetry constraints are imposed on the internal boundaries of panels and seams, while boundary constraints are applied to guarantee smooth and production-friendly edges. A hybrid boundary optimization strategy, which combines geometric constraints with B-spline fitting, is then utilized to refine the generated 2D patterns. Comprehensive experimental evaluations demonstrate the superiority of the proposed method. On a self-constructed dataset, it achieves an impressive 99.99% segmentation accuracy, and on cross-domain models, the accuracy reaches 99.91%. Moreover, compared with conventional approaches, the training time is reduced by 34%. For dresses and T-shirts, the generated patterns exhibit 100% structural similarity to template patterns, significantly outperforming the compared methods. Although the proposed method results in a slightly higher stretching ratio (ranging from 0.0157 to 0.0378) compared with the baseline methods (0.0112–0.0189), it ensures well-organized panel layouts and smooth boundaries, strictly adhering to industry standards and effectively preventing cutting errors caused by irregular shapes. By maintaining regular panel layouts and enforcing geometric constraints explicitly, the generated patterns preserve high fidelity during 3D-to-2D flattening while meeting industrial production standards.

Keywords

Garment mesh model, example-based approach, manufacturing constraint, graph neural network (GNN), pattern generation

The apparel industry is undergoing a significant transformation, shifting from traditional manual techniques to digital and intelligent garment production methods. Pattern-making, a critical component of this process, directly affects the quality and market competitiveness of the final product. Conventional manual pattern-making depends heavily on the expertise and skills of pattern-makers, leading to extended production cycles, low efficiency, and inconsistent pattern accuracy. These approaches struggle to meet the dynamic requirements of the modern apparel market. With advancements in computer technology, computer-aided design (CAD) systems have become widely adopted in the apparel industry,[1–3] partially improving pattern-making efficiency. However, most existing CAD systems still

[1]Zhejiang Sci-Tech University, School Computer Science and Technology (School of Artificial Intelligence), Hangzhou, China
[2]Zhejiang Provincial Innovation Center of Advanced Textile Technology, Shaoxing, China
[3]Zhejiang Sci-Tech University, International Institute of Fashion Technology, Hangzhou, China

Corresponding authors:
Yao Jin, 1. Zhejiang Sci-Tech University, School Computer Science and Technology (School of Artificial Intelligence), Hangzhou 310018, China.
Email: jinyao@zstu.edu.cn

Huaxiong Zhang, 1. Zhejiang Sci-Tech University, School Computer Science and Technology (School of Artificial Intelligence), Hangzhou 310018, China.
Email: zhxhz@zstu.edu.cn

Llli He, 1. Zhejiang Sci-Tech University, School Computer Science and Technology (School of Artificial Intelligence), Hangzhou 310018, China.
Email: llhe@zju.edu.cn

require substantial manual input, such as line drawing and dimension annotation, which limits production efficiency. Moreover, manual operations remain error-prone and provide only marginal efficiency improvements when addressing complex styles and diverse design demands. In addition, increasing consumer demand for personalized garments has driven a shift toward small-batch, multivariety production, requiring apparel companies to rapidly adapt to market changes and complete the design-to-production process within tight timelines. Traditional pattern-making methods are inadequately equipped to meet these evolving market demands, underscoring the urgent need for automated garment pattern generation.

Despite the apparel industry's ongoing shift from traditional manual techniques to digital and intelligent production, pattern-making remains a critical determinant of garment quality and market competitiveness. While significant progress has been made in automating 2D garment pattern generation, most existing methods still face substantial limitations. Parametric approaches[4] often rely on predefined prototypes and require extensive manual tuning to adapt to diverse designs, limiting their flexibility and innovation potential. Image-based methods,[5] although capable of capturing visual structures, struggle with complex 3D shapes and occluded regions, making them unsuitable for intricate or layered garments. Point cloud-based techniques[6] offer promising geometric insights but suffer from low topological resolution in high-curvature areas, leading to structural inaccuracies. Mesh-based methods,[7] while preserving detailed geometry, frequently produce patterns with distorted boundaries, irregular shapes, or excessive panel counts, failing to meet professional standards. Overall, the lack of a unified framework that integrates semantic understanding, geometric fidelity, and practical design constraints continues to hinder the development of robust and fully automated pattern generation systems.

To overcome these limitations, this paper focuses on mesh-based approaches and proposes an example-based framework that combines garment semantic segmentation with flattening strategies. By using standardized garment examples as references, the method guides the entire pattern generation pipeline, including semantic segmentation and pattern layout, addressing the shortcomings of conventional, example-free approaches. The approach employs a lightweight sparse graph transformer,[8,9] incorporating a global virtual node to enhance attention modeling. This enables multiscale feature extraction while maintaining low computational costs. In addition, a flattening algorithm was designed to enforce symmetry and boundary constraints, ensuring that the resulting patterns adhere to technical standards while preserving garment aesthetics and body symmetry. Overall, this paper introduces three key innovations, each contributing equally to the advancement of intelligent garment pattern generation.

1. *Automated example-based and craftsmanship-driven pattern generation*: This paper introduces an exemplar-based methodology that autonomously generates 2D garment patterns that adhere to traditional craftsmanship standards directly from 3D mesh inputs. By translating geometric constraints into manufacturable templates without manual intervention, this approach bridges the gap between digital design and artisanal expertise, ensuring production-ready patterns.
2. *Dynamic graph neural networks for enhanced garment semantic segmentation*: A novel method for garment segmentation is introduced, utilizing dynamic graph neural networks (GNNs). This approach integrates multiscale face adjacency graph (FAG) encoding with boundary-aware optimization modules to achieve high precision in delineating segmentation boundaries on complex garment surfaces. The method addresses the limitations of conventional techniques in modeling free-form deformations, delivering topologically coherent and visually natural segmentations for intricate 3D shapes.
3. *Manufacturing-constrained dual optimization for industrial-grade patterns*: An optimization algorithm incorporating symmetry and boundary line constraints is proposed. This approach combines geometric shape constraints with craftsmanship heuristics to systematically optimize industrial applicability metrics, such as sewing loss control and symmetry balance. By aligning 3D-to-2D flattening accuracy with production-ready specifications, the method generates 2D garment patterns that meet both technical and aesthetic requirements for real-world manufacturing.

Related work

Garment pattern generation

Researchers have explored a variety of methods aimed at automating the generation of 2D garment patterns. As indicated by Table 1, these methods can be broadly categorized into four primary types: parametric, image-based, point cloud-based, and mesh-based approaches.

Parametric methods enable designers to efficiently create customized garment patterns by adjusting the parameters, leveraging the strong correlation between the base prototypes and these parameters. Zhou et al.[4] developed parametric systems in AutoCAD using single- or double-circular arc fitting techniques. By defining constraints and parameter limits, these systems produce variant patterns, improving efficiency.

Table 1. Overview of the current state of garment pattern generation technologies

Garment pattern generation method	Advantages	Disadvantages
Parametric methods	Requires only key parameter adjustments for rapid pattern generation, user-friendly	Relies on predefined templates, limiting innovation in silhouette design
Image-based methods	Extracts structured pattern parameters directly from garment images, convenient data acquisition	Sensitive to occlusions, limited precision in detail reconstruction
Point cloud-based methods	Preserves 3D structural information effectively, suitable for complex surfaces	Lacks topological connectivity, prone to data redundancy in high-density regions
Mesh-based methods	Fully retains geometric and topological information, ideal for detailed modeling	Often ignores pattern-making technical standards, practicality is limited

Wang et al.[11] proposed a fuzzy neural network model that uses body dimensions as input to generate 2D garment pattern parameters based on fabric properties and fit requirements, achieving multiobjective optimization for personalization. Jin et al.[12] introduced an automated pattern generation method using parametric formulas implemented in Python. By classifying the curve parameters and developing three fitting algorithms, this method supports personalized pattern creation, with tests demonstrating significant time and resource savings. Korosteleva and Sorkine-Hornung[13] presented GarmentCode, a domain-specific language for garment modeling that employs object-oriented programming for the hierarchical component design. This language enables customization through parameter adjustments and supports automated editing, fostering creative exploration. However, these methods often depend on predefined prototypes, requiring iterative parameter adjustments to achieve desired shapes, which may limit structural innovation. Although GarmentCode expands generation capabilities, its reliance on programming skills restricts its broader adoption.

Image-based methods use machine learning and computer vision to extract structural features from 2D garment images and convert them into digital pattern-making parameters. Chen et al.[5] developed a hierarchical system that integrates Kinect scanning and Bayesian inference to detect garment components from images, enabling automatic template stitching for 3D reconstruction, although it does not generate 2D patterns. Yang et al.[14] proposed a single-view 3D garment reconstruction method that segments garments using graph-cut algorithms, extracts contours and wrinkles through edge detection and curve fitting, and employs garment simulation to produce garment patterns. Gou et al.[15] introduced a multilayer perceptron (MLP) classification model that parses pattern diagrams using multicolor line features, achieved through color space segmentation and structural feature quantization; however, its output is not yet integrated with automated pattern generation. Liu et al.[16] presented Sewformer, a two-stage Transformer-based network that processes garment layouts and panel edges, utilizing a visual encoder for step-by-step reconstruction and a seam similarity matrix to predict stitching. These methods achieve high automation with minimal manual intervention but rely heavily on 2D visual data, struggling with complex 3D structures, such as curved surfaces and layered seams. Occluded areas are frequently mispredicted, limiting their applicability to intricate designs. To address this, Chen et al.[17] introduced Panelformer, a Transformer-based model that reconstructs patterns from 2D images by analyzing symmetric panels and predicting occluded parts from visible ones, using data augmentation to enhance generalization. Despite reducing occlusion-related errors, it still faces challenges with complex garment structures.

Point-cloud-based methods integrate geometric and topological analysis with deep learning to facilitate 3D reconstruction and feature extraction from garment point cloud data. Korosteleva and Lee[6] combined 3D point cloud topological attention with recurrent neural network (RNN) mesh modules. High-level decisions parse global garment structures, whereas RNNs refine local details for pattern reconstruction, bypassing the flattening steps. Huang et al.[18] enhanced the NeuralTailor framework by incorporating edge loss refinement and high-order Bézier curve modeling to achieve precise and smooth contour fitting, thereby improving the engineering adaptability of patterns without requiring flattening steps. However, these methods often exhibit low topological resolution in high-curvature regions, such as underarm areas, resulting in structural deformation during reconstruction.

Mesh-based methods establish 3D-to-2D mappings through geometric feature analysis and physical constraint optimization of garment mesh models. Bang et al.[7] proposed to extract seam features using

predefined human body templates, determining segmentation boundaries (e.g., cuffs) via projection and refining edges through implicit optimization techniques. This approach generates sewable 2D garment patterns through geometric flattening. Pietroni et al.[10] developed a cross-field aligned with the principal curvature directions of the surface, ensuring smooth transitions through global smoothing optimization. Using graph theory, this method dynamically adjusts segmentation paths, prioritizing the merging of developable surfaces in regions with low Gaussian curvature. During flattening, an affine transformation model accounts for the warp and weft directions, with Jacobian matrices quantifying the fabric stretch and shear deformation, enabling surface flattening while preserving the mechanical properties of the fabric. Xiao et al.[19] extracted body feature points through the geometric analysis of cross-sectional curves and achieved structure-preserving 3D surface flattening using a mass–spring system, generating customized 2D garment patterns with empirically validated edge compensation strategies. Nevertheless, these methods frequently produce 2D patterns with nonsmooth boundaries, irregular shapes, and excessive panel counts.

Semantic mesh segmentation

Semantic segmentation of 3D garment meshes plays a crucial role in generating accurate and structurally meaningful 2D patterns, as it enables the identification of key garment components such as front and back panels. Various methods have been proposed to address this task but targeting various applications, including data-driven learning approaches and optimization-based techniques. Among them, conditional random fields (CRFs),[20,21] a probabilistic graphical model based on Markov random field properties, enable 3D mesh semantic segmentation by constructing unary (patch geometric features) and pairwise (adjacency relationships) energy functions, optimized with weights for the normalized area and edge length. These methods effectively optimize the patch-level topology by leveraging global geometric feature correlations, but they face challenges with nonuniform mesh density and complex surface structures. Liu et al.[22] applied CRF-based segmentation to garment models, although their results emphasized garment components rather than critical garment pattern elements, such as front and back panels. This highlights a key limitation: while traditional approaches can capture coarse-level structure, they lack the precision required for industrial-grade pattern generation.

Recent advancements in deep learning, particularly in 3D mesh semantic segmentation using deep convolutional neural networks (CNNs), have significantly improved accuracy by learning robust mesh representations adaptable to diverse 3D models. Guo et al.[23] introduced a method for 3D mesh labeling using deep CNNs, which automatically learns adaptive mesh representations through supervised training, effectively addressing the limited generalization of traditional low-level handcrafted features. Similarly, Xu et al.[24] employed a dual-layer CNN for tooth–gingiva separation and tooth identification, thereby reducing computational costs through boundary-aware simplification. However, applying these methods directly to garment segmentation remains challenging due to the complex topology and high-density meshes of the garment models, which increase the computational complexity and impede real-time performance. Moreover, existing methods struggle to model nonlinear deformations, such as fabric draping and folds, limiting their adaptability to dynamic structural relationships in free-form garments.

Example-based garment pattern generation

As a foundational example for 3D-to-2D parametric conversion, the accuracy of garment pattern in structural feature representation directly affects pattern-making efficiency and process adaptability. Existing example-based methods such as image-to-model generation or basic-block modification typically split garments into modules.[5,25] The former requires exhaustive definitions for each module (e.g., collar types), whereas the latter relies on manual design and parameter tuning, yet neither generates patterns directly usable in industrial production. Pattern generation methods[10] without exemplar references often produce inconsistent panel counts and fail to extract/optimize boundary geometry, resulting in uneven edges. This paper proposes defining a unified model per garment type using graph structures as shown in Figure 1. It parameterizes geometric features (e.g., seam lengths) and topological relationships (e.g., stitching logic) into patch stitching graphs (PSGs). By adapting a single structural template across sizes, the method avoids detailed design for each style, ensures consistent panel counts, and optimizes boundary geometry to address panel mismatch and edge distortion in nonexemplar-driven approaches.

Geometric properties

The PSG facilitates parametric modeling by converting the geometric and topological information of garment exemplars into guiding rules. Each 2D garment pattern piece, represented as a node, is geometrically encoded through a dual mechanism. First, index consistency is established using boundary labels derived from garment semantic segmentation, ensuring the precise mapping and reconstruction of boundaries during the

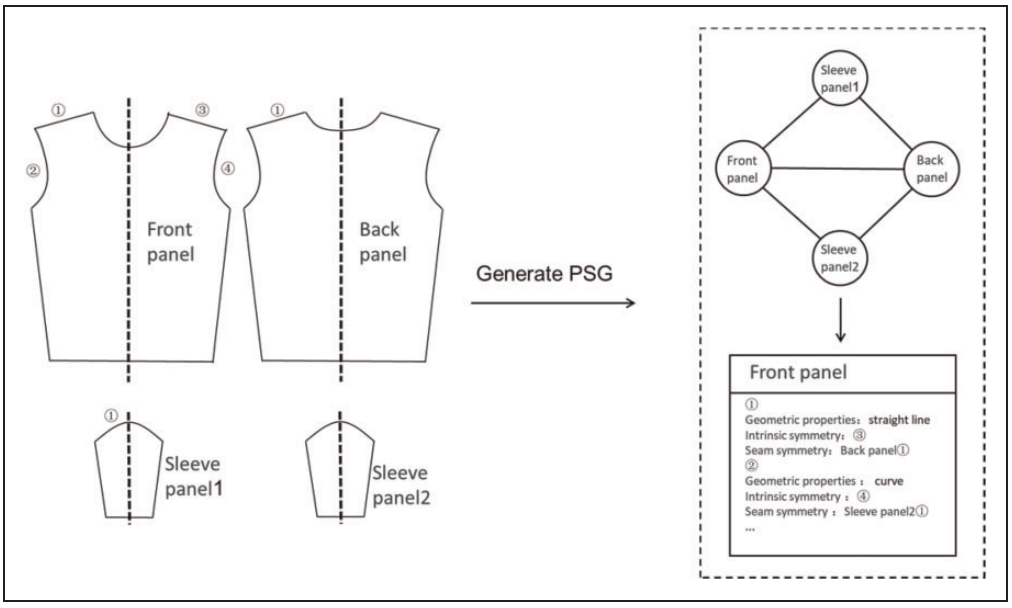

Figure 1. Patch stitching graph.

parametric process through unique identifiers. Second, a domain-specific representation strategy is employed: regular edges, such as cuffs and pant legs, are defined using straight boundary lines, whereas complex shapes, such as waist and hip contours, are modeled parametrically with B-spline curves. Straight boundary endpoints provide rigid constraints, whereas curved boundary control points allow flexible shape adjustments. This hybrid representation preserves the geometric constraints in critical regions while enabling smooth 3D-to-2D surface mapping through parametric optimization, ensuring that the patterns conform to the human body contours and meet industrial production standards.

Symmetry properties

Symmetry is the cornerstone of garment pattern design, balancing esthetics and functionality. The PSG accurately captures symmetry through coordinated constraints in both 2D and 3D spaces. In the 2D plane, the patterns exhibit mirror symmetry along the central axis, as demonstrated by the axial symmetry of the left and right shoulder lines in the front panel as illustrated in Figure 1. This property simplifies the pattern design and enhances the visual coherence. In 3D space, vertex reflection symmetry constraints on segmentation boundaries ensure geometric consistency during sewing, such as the seamless alignment of the front and sleeve panel boundaries. This dual-symmetry mechanism enhances the reliability of the 3D-to-2D pattern conversion and minimizes manufacturing errors, thereby reducing adjustment costs. By defining symmetry attributes within the PSG, the parameterization process automatically applies exemplar symmetry rules, eliminating deviations common in manual annotation and significantly improving the efficiency and accuracy of digital pattern generation.

Example-driven parametric rule generation

Garment exemplars guide parametric modeling by leveraging structured features. The PSG analyzes the garment semantic segmentation results of 3D models, identifying boundaries where adjacent faces have distinct labels as potential stitching edges. Valid stitching combinations are filtered on the basis of predefined process rules. For instance, when an edge is detected between the faces corresponding to the front and sleeve panels, the PSG automatically generates the stitching edge with associated attributes, such as the curve type and control point count. This process translates the design expertise into computable constraint rules, providing clear objective functions for parametric optimization. The geometric and symmetry properties of the exemplars are encoded as mathematical constraints for pattern unfolding, ensuring that the parametric results exhibit traditional craftsmanship characteristics while accommodating personalized design requirements. This approach achieves a seamless integration of intelligent pattern generation with industrial production needs.

Recognition of garment pieces

Semantic segmentation of garment models

The geometric complexity of 3D garment models, characterized by irregular surfaces, multiscale features, and

nonrigid deformation properties, renders traditional rule-based or handcrafted feature segmentation methods ineffective for processing such nonlinear structural data. Accurate mapping from 3D models to 2D garment patterns requires dividing garment surfaces into semantically coherent units, such as sleeves and front panels, while preserving topological and geometric consistency across adjacent patch boundaries.

In response to these difficulties, this paper introduces a GNN segmentation method based on face-edge adjacency graphs as illustrated in Figure 2. This method transforms triangular meshes into graph-structured data, representing each triangular face as a node and defining edges by shared boundaries between adjacent faces. Node features incorporate geometric and contextual information, including centroid coordinates, normal vectors, contextual label features, curvature, and principal component analysis (PCA) descriptors.[20,28] Edge features capture geometric relationships between adjacent faces, including midpoint coordinates, edge length, convexity/concavity indicators, and dihedral angles.

These diverse features are mapped into a unified high-dimensional embedding space using a MLP. This paper designs an encoder–decoder architecture with graph transformers to construct a face classification probability prediction model within this feature space. By leveraging sparse multihead attention mechanisms, the network preserves local details while capturing large-scale semantic relationships, producing patch category probability distributions for each face. This approach enables intelligent segmentation of 3D garment models, supporting the generation of topologically consistent 2D garment patterns. Through this method, this paper achieves accurate and efficient segmentation, overcoming the limitations of traditional approaches.

Sparse graph transformer for large-scale meshes

In mesh-based graph structures, nodes are only connected to their local neighborhoods, meaning that each node interacts with only a small number of nearby nodes. This inherent sparsity implies that when constructing an attention mechanism, it is unnecessary to compute interactions between all node pairs. However, relying solely on local attention mechanisms may lead to information loss due to the neglect of long-range dependencies. Although mesh structures are naturally sparse, in high-resolution garment mesh models, the number of nodes can be extremely large, often reaching tens of thousands in highly detailed designs. If a conventional attention mechanism is employed, the computational complexity becomes quite high, to some extent limiting the model's practical applicability.

To address this issue, this paper introduces a lightweight attention architecture that incorporates learnable virtual nodes. These virtual nodes are initialized as featureless vectors and act as central communication hubs, establishing bidirectional connections with all real nodes. Real nodes connect exclusively to virtual nodes, while the virtual nodes aggregate global features and disseminate information. Through parameterized aggregation functions, virtual nodes dynamically integrate local features from each node, producing compressed global features Z_g. These features are then distributed back to the real nodes. This sparse design maintains global semantic coherence while eliminating

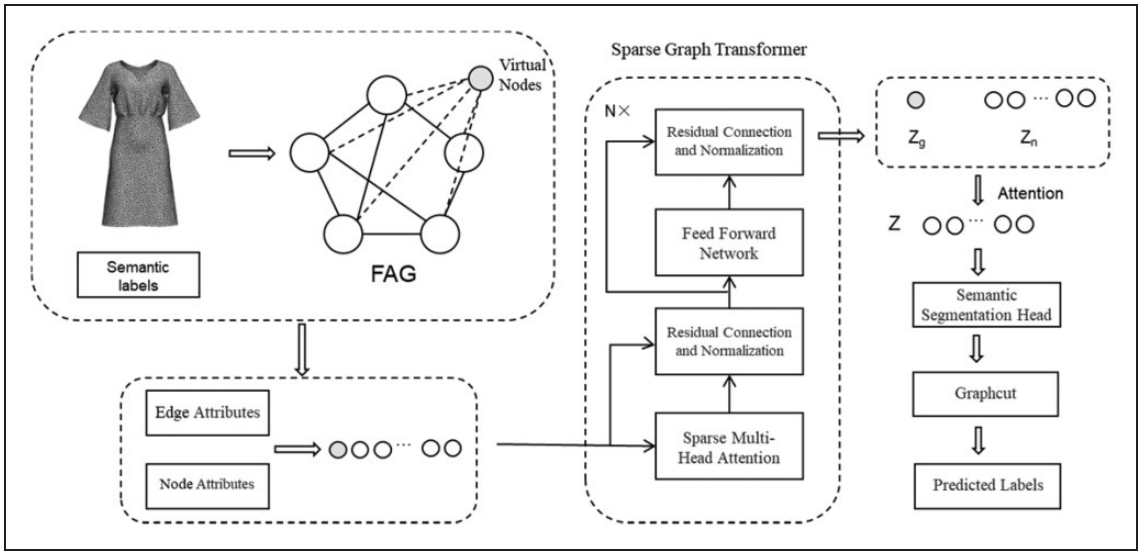

Figure 2. The network architecture.

direct node-to-node interactions, significantly improving the computational efficiency.

To mitigate the weight imbalance during feature fusion, which may occur from directly concatenating local node features Z_n and global graph features Z_g a dynamic attention fusion mechanism is proposed. Attention weights for both feature types were computed using a learnable parameter matrix W, ensuring balanced integration and enhanced model performance:

$$[A_n, A_g] = W([Z_n, Z_g]) \tag{1}$$

Subsequently, weight normalization is accomplished using the softmax function:

$$[A_n, A_g] = softmax([Z_n, Z_g]) \tag{2}$$

Finally, an adaptive feature representation is generated through a weighted fusion process:

$$Z = A_n Z_n + A_g Z_g \tag{3}$$

This approach allows the model to dynamically adjust the balance between local details and global context based on the input features. In contrast to fixed weights or strategies that rely on single-feature selection, it improves the flexibility of feature expression while preserving computational efficiency.

Loss function

Garment semantic segmentation can be conceptualized as a multicategory node classification task that targets the mesh faces. To accomplish this, the garment semantic segmentation module utilizes a MLP to classify the feature vector Z associated with each face, producing a probability distribution matrix of dimensions $N_f \times N_c$, where N_f represents the total number of faces and N_c denotes the number of garment pattern categories. This matrix reflects the confidence scores for each face belonging to specific pattern types. For the classification task, a standard cross-entropy loss function was employed to measure the discrepancy between the predicted probabilities and ground truth labels, optimizing the model's performance:

$$L_{cls} = \frac{1}{N_f} \sum_{i=0}^{N_f} y_i \log(\hat{y}_i) \tag{4}$$

where y_i and $\hat{y}_i$ represent the ground truth label and the probability vector outputted by the garment semantic segmentation head for the ith face, respectively.

To enhance semantic coherence among adjacent faces, a structural coherence loss is introduced. This loss function quantifies the feature similarity between neighboring faces via an edge-level link prediction task. Specifically, for each nonboundary edge, the inner product of the feature vectors from its two adjacent faces is calculated, and a link score s is obtained using the sigmoid function:

$$s = \sigma(Z^T Z) \tag{5}$$

where σ denotes the sigmoid function. The loss function is then defined as the binary cross-entropy between the link scores and the adjacency relationships:

$$L_{sc} = \frac{1}{N} \sum_{i=0}^{N} [-\alpha \log(s) - (1-\alpha)\log(1-s)] \tag{6}$$

where N represents the total number of nonboundary edges in the mesh model, and α is an indicator function that equals 1 if the labels of adjacent faces are consistent and 0 otherwise.

Boundary optimization

Precise boundary delineation in garment patch segmentation is essential for ensuring the feasibility of subsequent garment pattern generation and production processes. While GNNs provide initial segmentation results, relying solely on neural network predictions or geometric attributes may fail to resolve boundary ambiguities, particularly in flat regions. To address this challenge, this paper employs the GraphCut algorithm[26] to refine the segmentation boundaries by integrating semantic predictions with geometric continuity constraints.

Specifically, a dynamic transition zone is established around the preliminary segmentation boundaries. Within this zone, a dual-modality weight assessment system evaluates each face, measuring semantic consistency based on class confidence derived from GNN outputs and local smoothness using geometric features, such as surface curvature and angles between the normal vectors of adjacent faces. The GraphCut algorithm describes an energy function that maximizes semantic consistency while ensuring that the boundaries align with the physical seam characteristics of the garment patterns. This approach excels in resolving boundary ambiguities in regions with subtle geometric features, such as sleeves and hems, effectively eliminating jagged segmentation artifacts. The resulting boundaries adhere to the natural, streamlined structure of the garment while preserving semantic coherence.

Pattern flattening

Following the segmentation of a 3D garment model into subpatches, the subsequent step involves parametrizing and unfolding these patches to generate 2D garment patterns. This process must satisfy three key requirements. First, it must preserve the anisotropic fabric properties while maintaining distinct stretching characteristics in the warp and weft directions to prevent physically implausible uniform deformation during flattening. Second, it must strictly adhere to garment craftsmanship standards for pattern boundaries, ensuring that straight lines remain straight and curved boundaries are smooth to avoid jagged or irregular distortions that could impair cutting accuracy. Third, it must enforce multilevel symmetry constraints by implementing axisymmetric optimization for individual patterns and ensuring geometric symmetry at paired sewing edges.

To achieve these objectives, this paper proposes a comprehensive energy function that integrates multiple constraints:

$$E_{pattern} = \omega_{boundary}(E_{straight} + E_{curve}) + \omega_{sym}(E_{inner} + E_{seam}) + \omega_{\text{stretch}} E_{stretch} + \omega_{rigid} E_{rigid} \tag{7}$$

where ω denotes the weighting coefficients for each energy term. Empirically, the weights for the energy terms are set as $(\omega_{boundary}, \omega_{sym}, \omega_{stretch}, \omega_{rigid}) = (5, 5, 5, 1)$. The stretching energy term $E_{stretch}$ and the rigid transformation energy term E_{rigid} are developed following the methodology proposed by Pietroni et al.[10] This approach effectively preserves the anisotropic properties of the fabric by independently penalizing the stretch deformations along the u and v directions, as well as the shear deformations. Compared with conventional uniform deformation constraints, this energy formulation significantly enhances the computational efficiency during the parameterization process. In addition, it mitigates nonrigid deformations through the rigid transformation energy, thereby ensuring the controllability of local deformations.

To address the limitations in the current garment pattern standardization, such as boundary deformation, two key improvements are introduced. First, a hybrid boundary constraint energy was developed, combining straight lines and B-spline curves to enable precise control over the garment pattern boundary morphology. Second, symmetry constraints are implemented to balance seam symmetry optimization with esthetic and functional requirements. The following sections elaborate on the innovative designs of these boundary and symmetry constraints.

To enhance the precision and consistency of the B-spline curves, particularly in aligning their endpoints with the specified boundary endpoints, the Lagrange multiplier method is employed to solve the equality-constrained optimization problems. By incorporating Lagrange multipliers, the geometric constraints are seamlessly integrated into the optimization objectives, effectively controlling the shapes and positions of the spline curves. The goal is to determine control points $P_0, P_1,\ldots,P_n$ that satisfy the given data point Q_0, $Q_1,\ldots,Q_m$ and constraints:

$$\begin{bmatrix} 1 & 0 & -1 & 0 \\ 0 & 1 & 0 & -1 \end{bmatrix} \begin{bmatrix} Q_0 \\ Q_m \\ P_0 \\ P_n \end{bmatrix} = \begin{bmatrix} 0 \\ 0 \end{bmatrix} \tag{8}$$

which can be abbreviated as $TP = y$.

Defining the boundary and symmetry constraints requires establishing equations with the straightish boundary lines and symmetric axes. Incorporating the unknown coefficients of these equations as hidden variables in the optimization process could increase the nonlinearity and solution complexity. To mitigate this, a two-stage approach is adopted. In the first stage, the constraints are relaxed, focusing solely on optimizing the stretching energy ($E_{stretch}$) and the rigid transformation energy (E_{rigid}) using a method similar to Pietroni et al.[10] This stage runs for five iterations and produces an initial result. In the second stage, the previously undetermined hidden variables are resolved, and the full energy function (7) is optimized over 15 iterations. This strategy reduces nonlinearity, simplifies the optimization process, and preserves the fabric's anisotropic properties while ensuring precise adherence to manufacturing specifications, thereby guaranteeing that the final garment patterns meet high-quality design and production standards.

Pattern boundary constraints

To improve the quality of the 2D garment pattern boundaries, they were classified into two categories: straight lines and smooth curved lines (represented as B-spline curves). The aim is to ensure that these boundaries closely conform to their idealized forms, consistent with garment patterns typically generated by CAD software. Boundaries are first categorized by analyzing the geometric attributes derived from the example-based data and determining which segments should be straight or curved. Subsequently, the equations for each boundary type were formulated, and the positions of the boundary vertices were optimized using algorithms to achieve the desired fit.

Straight line boundary constraints. For straight line boundaries, the optimization objective is to ensure that all mesh vertices (x_i, y_i) on the pattern boundary lie on the same straight line $y_i = mx_i + c$. As the coefficients m and c of the line equation are initially unknown, they can be determined by fitting them to the boundary vertices of the results obtained from the initial stage, as previously discussed.

To elaborate, an energy function is constructed as the sum of the squared distances from each boundary vertex to the intended straight line. The process of line fitting is achieved by minimizing this energy function. Initially, the line equation is established utilizing all vertices positioned along the boundary:

$$(m, c) = \text{argmin} \left\| \sum_{i=1}^{n} (y_i - (mx_i + c)) \right\|_2^2 \tag{9}$$

where n represents the number of vertices on the boundary. Based on the fitted straight line equation, the linear constraint is then constructed as

$$E_{straight}(\boldsymbol{x}, \boldsymbol{y}) = \left\| \sum_{i=1}^{n} (y_i - (mx_i + c)) \right\|_2^2 \tag{10}$$

Spline curve boundary constraints. The key advantage of B-spline curves is rooted in the distinctive design of their basis functions. Each basis function exclusively affects parameter intervals (defined by the knot vector T), thereby ensuring that the effect of control points is precisely localized. Modifying a single control point alters the curve's shape solely within its corresponding parameter interval, leaving other segments unaltered. This local support characteristic, combined with the gradual distribution of the parameter $t \in [0, 1]$, ensures global smoothness while permitting local adaptability.

In this paper, a cubic B-spline curve (with $k = 3$) is utilized for boundary fitting, achieving a harmonious balance between computational efficiency and fitting precision. The knot vector T is configured with a length of 5 (typically sufficient for modeling various curves, given that the boundary curve is generally smooth and fair), where intermediate knot positions are established by identifying curvature peaks along the curve, and other knots are determined by segment midpoints. During the construction of T, to maintain the open knot vector property, the number of repeated knots at both ends must correspond to the B-spline order k. As a result, two additional repeated knots are added to each end of T.

Upon constructing the knot vector, the vertex set Q is employed for interpolation fitting to determine the control points P of the B-spline curve. By formulating and minimizing an energy function $E_{bspline}$ that combines curve smoothness and vertex fitting error, both the control points and boundary vertex positions are optimized to achieve precise fitting. The energy function is expressed as follows:

$$E_{bspline}(P, Q) = \left\| \sum_{i=1}^{n_Q} \left[\sum_{j=1}^{n_P} P_j N_j(t_i) - Q_i \right] \right\|_2^2 \tag{11}$$

where $N_j(t_i)$ is the basis function at parameter t_i, and n_Q and n_P are the numbers of vertex set Q and control point set P, respectively.

To further enhance curve smoothness, constraint terms related to the first- and second-order derivatives of the curve are incorporated into the energy function, effectively suppressing excessive bending and ensuring a natural appearance. The comprehensive energy function for the spline curve is formulated as

$$\begin{aligned} E_{curve}(P, Q, t) = {} & E_{bspline}(P, Q) + \alpha \| r^{(1)}(t) \|_2^2 \\ & + \beta \| r^{(2)}(t) \|_2^2 \end{aligned} \tag{12}$$

where α and β are adjustable weights, both set to 3 empirically in the experiments, and $r^{(1)}(t)$ and $r^{(2)}(t)$ are the first- and second-order derivatives of the B-spline curve, respectively.

Pattern symmetry constraints

Symmetry constraints are pivotal in geometric modeling, as they enhance aesthetic appeal and structural consistency while streamlining the modeling process. In this paper, symmetry constraints are selectively applied to key nodes along boundaries, with other vertices achieving symmetry through boundary constraints. Specifically, straight boundaries enforce symmetry at their endpoints, whereas curved boundaries maintain symmetry among their control points. These constraints are implemented in two forms: internal pattern symmetry and reflective symmetry at seams. For nonsymmetric regions or boundaries where symmetry is not required, these constraints are omitted, enabling the proposed method to naturally accommodate asymmetric designs without imposing unnecessary restrictions.

Single pattern symmetry. To ensure internal pattern symmetry, constraints are implemented to enforce symmetrical arrangements of model components. For straight boundaries, endpoints maintain strict symmetry, and

linear constraints propagate this symmetry to other vertices. For boundaries defined by spline curves, symmetry is attained by restricting all control points to symmetrical configurations with respect to predefined symmetry axes. The internal symmetry energy function is formulated as follows:

$$E_{inner}(X) = \left\| \sum_{i=0} [X_i^1 - R(X_i^2)] \right\|_2^2 \tag{13}$$

where X_i^1 and X_i^2 denote key nodes on two symmetric boundaries, and R represents the symmetric transformation,[27] which can be determined precisely by fitting it to the results derived from the initial flattening stage of the process.

Seam reflective symmetry. In pattern design, attaining reflective symmetry at seams is essential to guarantee seamless transitions and uphold the aesthetic coherence between stitched components. However, nonlinear parametrization can result in the misalignment of seam vertices in 2D space. To address this issue, optimal reflection transformations are calculated to reinstate symmetric relationships. To achieve a balance between flexibility and smoothness, reflective symmetry constraints are applied solely to key seam nodes, while other boundary vertices are dynamically adjusted through optimization. This method maintains symmetry while preserving natural shape continuity. The seam energy function is defined as follows:

$$E_{seam}(X) = \left\| \sum_{i=0} \left[(X_i^1 - X_i^{1\prime}) + (X_i^2 - X_i^{2\prime}) \right] \right\|_2^2 \tag{14}$$

where $X_i^{1\prime}$ and $X_i^{2\prime}$ denote the reflection counterparts of X_i^1 and X_i^2.

Numerical solution

To address the energy minimization problem outlined in (7) while adhering to the equality constraints in (8), an augmented Lagrangian objective function is formulated as follows:

$$L = E_{pattern} + \lambda_0(Q_0 - P_0) + \lambda_n(Q_m - P_n) \tag{15}$$

where λ_0 and λ_n denotes Lagrange multipliers.

To find the optimal control points P^* and multipliers λ^*, the constrained optimization problem is transformed into an unconstrained one. By differentiating the objective function with respect to P and λ, and setting the derivatives to zero, the Karush–Kuhn–Tucker (KKT) system is derived:

$$\begin{bmatrix} 2T^T T & A^T \\ A & 0 \end{bmatrix} \begin{bmatrix} P^* \\ \lambda^* \end{bmatrix} = \begin{bmatrix} 2T^T y \\ b \end{bmatrix} \tag{16}$$

Minimizing the energy term $\|E_{pattern}\|_2^2$ results in a least-squares formulation of the fundamental equation $A'x = b'$. To improve numerical stability, the regularization matrix A and vector b are constructed accordingly:

$$\begin{aligned} A &= A'^T * A' \\ b &= b'^T * b \end{aligned} \tag{17}$$

The final matrix A and vector b are employed to formulate the KKT system. By minimizing the Lagrangian function, both geometric constraints and physical properties are concurrently satisfied, ensuring that the generated spline curves adhere to design specifications while preserving smoothness and precision. The proposed method demonstrates robust performance and practical applicability in spline curve design, providing an efficient solution for optimizing complex geometric shapes in garment pattern generation.

Experiments and discussion

Implementation detail

Network setting. Experiments were conducted on a system equipped with an Intel i5-13600KF CPU, an NVIDIA RTX 3070 GPU, and 16 GB of RAM, capable of efficiently processing large-scale 3D data. For model training, the AdamW optimizer is utilized with an initial learning rate of 0.002, and momentum parameters β_1 and β_2 are set to 0.99 and 0.999, respectively. A dynamic decay strategy based on validation loss is implemented for learning rate scheduling: when the validation loss reaches a plateau, the learning rate is reduced by a factor of 0.5, with a minimum learning rate of 1×10^{-6} enforced.

Dataset construction. A dataset of 3D garments was built to meet the training needs for model segmentation, ensuring both variety and structural consistency. Figure 3 illustrates four common garment categories in this dataset: T-shirts, shirts, pants, and dresses. Each category includes 10 base garment patterns, each exhibiting distinct styles while adhering to a uniform structure. For dresses, the base pattern library provides 15 design variations, such as A-line and sheath, characterized by consistent attributes such as

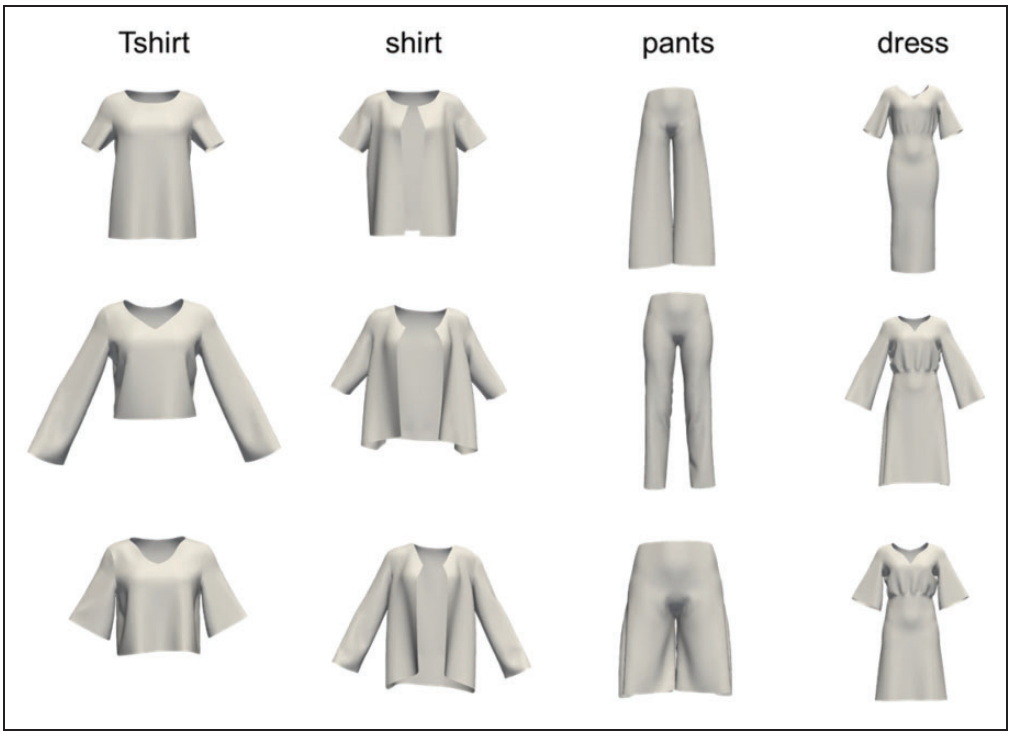

Figure 3. Several representative models in the dataset.

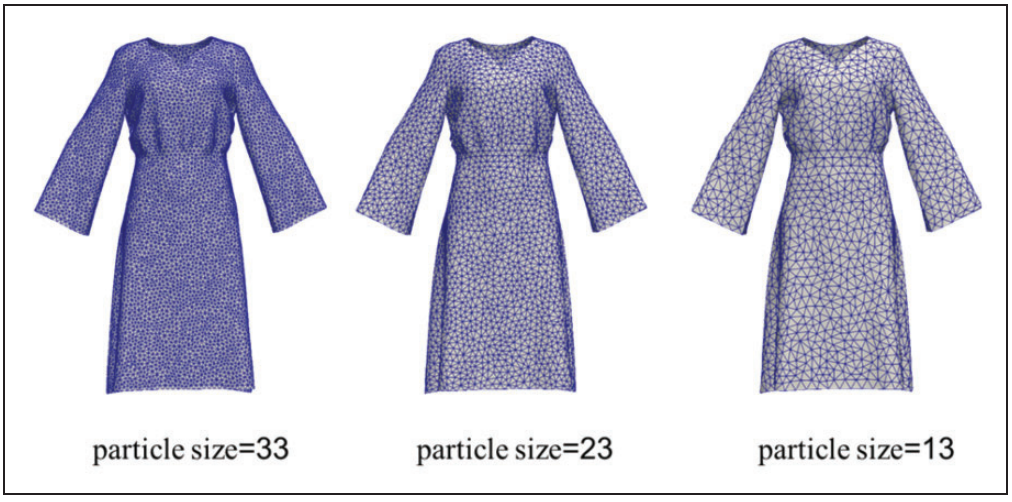

Figure 4. Dress models with different mesh particle sizes.

fixed seam counts and boundary type ratios. All patterns were created using the Style3D software, with mesh face counts limited to 15,000 to balance detail and computational efficiency during training.

To improve realism while preserving structure, topological variations were generated by modifying the parameters of the mesh particle system, which correspond to the number of vertices. As illustrated in Figure 4, for each base pattern across the 15 designs per garment category, dynamic adjustments to the particle size result in varied mesh vertex density distributions. These modifications preserve the underlying pattern topology, including seam types and connectivity, while effectively simulating real-world variations in garment fit and drape, ranging from loose to fitted styles. This process yields 150 topologically diverse 3D garment models per category, all of which retain the original seam types and counts. These variations cover a spectrum of garment patterns, including loose and fitted styles, and undergo geometric validation to

ensure 3D developability aligns with physical pattern-making constraints.

To ensure the dataset's quality and utility, each pattern is meticulously annotated. Specifically, every polygon face is labeled to denote its corresponding garment panel, enabling the algorithms to distinguish subtle differences between panels. This detailed annotation enhances the model's learning and improves segmentation accuracy.

For the segmentation experiments, 100 patterns from each garment category's 150 variants were assigned to the training set, with the remaining 50 reserved for the test set. The model underwent 300 training iterations to ensure thorough feature learning, thereby improving segmentation accuracy and robustness. To evaluate the effect of training set size, this paper conducted ablation studies using 150, 100, and 70 garment models per category. This paper found that using 70 models led to faster training but lower accuracy, whereas 150 and 100 models achieved very similar average accuracies, differing by only 0.003%. However, increasing the training set from 100 to 150 models caused the average training time to increase by approximately 24%, suggesting that 100 models offer a better trade-off between performance and computational efficiency.

Evaluation metrics. To comprehensively evaluate the performance of the proposed method in both semantic segmentation and garment pattern generation, this paper design a set of evaluation metrics across multiple dimensions.

For the performance of the semantic segmentation network, this paper mainly focus on two aspects: accuracy and inference efficiency (computational time). The accuracy is quantitatively measured using the following metric:

$$\text{Accuracy} = \frac{1}{N_{Mesh}} \sum_{i=0}^{N_{Mesh}} \frac{|\text{Correct faces}|}{|\text{Total faces}|} \tag{18}$$

where N_{Mesh} represents the number of mesh models in the test set. This metric reflects the proportion of correctly predicted garment components over the entire test set, serving as a key indicator for evaluating the quality of semantic segmentation.

For the quality assessment of generated garment patterns, this paper consider three main criteria: computational efficiency (time), structural consistency, and geometric deformation (stretching metric D). This multi-dimensional evaluation ensures that the generated results are not only efficient but also structurally and geometrically sound.

(1) Structural consistency metric. To evaluate the structural consistency of the generated garment patterns, in this paper we convert the fabric pieces obtained from garment model segmentation into face-edge graphs. Each fabric piece is represented as a node in the graph, and the seam edge connecting two pieces is treated as an edge. This representation effectively captures the spatial relationships and connectivity between different pieces. Next, we use a set of topological features to describe the face-edge graphs. These features include average degree, maximum degree, minimum degree, average clustering coefficient, variance and skewness of degree distribution, number of connected components, and average path length. These features are then dynamically normalized. Based on an improved Euclidean distance calculation method, the difference between two graphs is converted into a similarity percentage ranging from 0% to 100%, providing a clear measure of their structural similarity.

(2) Stretching metric.. This paper utilizes the stretching metric D to quantitatively assess geometric deformation during the flattening of garment patterns. The metric evaluates stretching quantity between 2D patterns generated by the proposed method and those produced by Pietroni et al.,[10] relative to their corresponding 3D garment meshes. This paper introduces a quantitative analysis model to evaluate UV-direction stretching ratios for each triangular face in the mesh. As shown in Figure 5, a 3D triangular face $A'B'C'$ is mapped to its 2D counterpart ABC through an affine transformation. To construct the parameterization framework, the centroid G of the triangle in 2D space and its offset points $G_u = G + (1,\ 0),\ G_v = G + (0,\ 1)$ along the u and v directions are introduced. Based on this setup, the stretching ratios r_u and r_v along the u and v directions are defined as follows:

$$r_u = \frac{s_u'}{s_u}, \quad r_v = \frac{s_v'}{s_v} \tag{19}$$

where $s_u = \|G_u' - G'\|$ and s_v, s_u', s_v' can be similarly derived. When $r > 1$, it indicates that the triangular face experiences stretching deformation in that parameter direction, whereas $r < 1$ indicates compression deformation. To systematically evaluate the overall stretch distribution characteristics of the three-dimensional clothing model, this paper adopts a statistical measurement method based on geometric deviation. The construction of this method is based on two fundamental criteria: first, the degree of stretching and compression deformation is uniformly represented in the form of squared differences; second, an area-weighted coefficient is introduced, allowing triangular

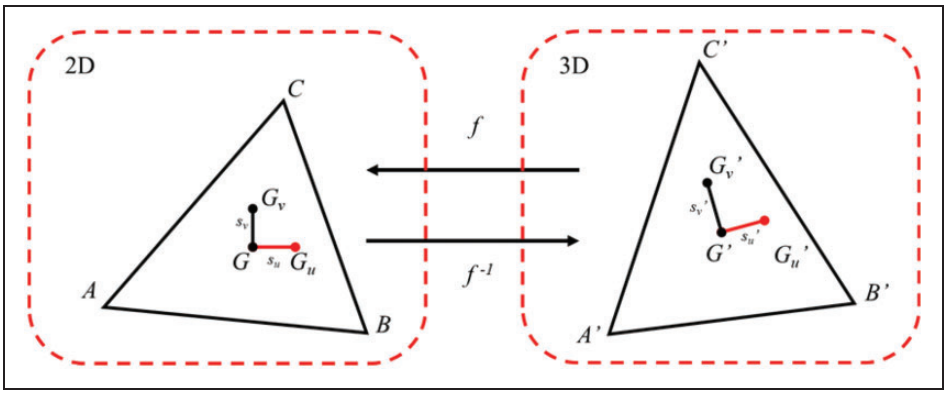

Figure 5. Illustration of the stretching metric *D*.

faces with larger surface areas to contribute more to the overall measurement results. The final stretching metric D is defined as

$$D = \frac{\sum_i A_i \sqrt{(r_{u,i}-1)^2 + (r_{v,i}-1)^2}}{A_{total}} \tag{20}$$

where A_i represents the area of the ith triangular face and A_{total} is the total surface area.

Validation of model component effectiveness

Structural coherence constraint loss. This paper experimentally evaluates the effect of structural coherence loss on enhancing semantic consistency among adjacent garment pattern panels. The results demonstrate that incorporating the structural coherence constraint loss leads to smoother boundary transitions between neighboring panels, significantly improving semantic consistency. Specifically, the average segmentation accuracy increased from 99.96% to 99.99%.

Figure 6 compares the segmentation outcomes before and after applying the application of structural coherence Loss. Prior to its integration, certain panels exhibited suboptimal garment semantic segmentation performance, with misclassifications particularly pronounced in boundary regions. After implementation, the model demonstrates significant improvements in maintaining semantic consistency across neighboring panels. These findings confirm that the structural coherence loss effectively mitigates isolated misclassified panels, aligning segmentation results more closely with the inherent structural characteristics of garment components.

Boundary optimization strategy. This paper evaluates the effectiveness of boundary optimization strategies by comparing segmentation results before and after their implementation. Prior to optimization, boundaries exhibit pronounced sawtooth artifacts and local ambiguities, leading to misclassifications of panels. As illustrated in Figure 7, optimized boundaries demonstrate significant improvements, characterized by smoother contours, effective elimination of sawtooth artifacts, and precise alignment with the natural structure of garments. All panels are accurately classified, resulting in a marked enhancement in semantic coherence. Experimental results confirm that the proposed hybrid optimization strategy effectively resolves boundary ambiguities, particularly in texture-deficient flat regions. While maintaining semantic consistency and geometric smoothness, the approach generates high-quality segmented garment patterns suitable for subsequent pattern-making and production processes. Postoptimization, the average boundary smoothness improves substantially, yielding notable enhancements in both the visual quality of segmentation outcomes and the accuracy of subsequent garment pattern generation.

Ablation analysis of key modules. To validate the efficacy of the key components within the sparse graph model, this paper designs hierarchical ablation experiments to independently evaluate the contributions of the global virtual node weighting module and the sparse attention mechanism, as well as their synergistic effects. As presented in Table 2, three experimental setups are employed: the full model, a streamlined model without the global virtual node weighting module (i.e., lacking dynamic attention fusion), and a baseline model utilizing conventional graph transformers.[8]

The experimental data yields several key insights. First, when the global virtual node weighting module is removed, the model's accuracy experiences a slight decline of 0.01 percentage points. This observation underscores the module's crucial role in enhancing the capture of intricate local details, such as garment seams and folds, by dynamically fusing multiscale contextual features. Second, the baseline model, which

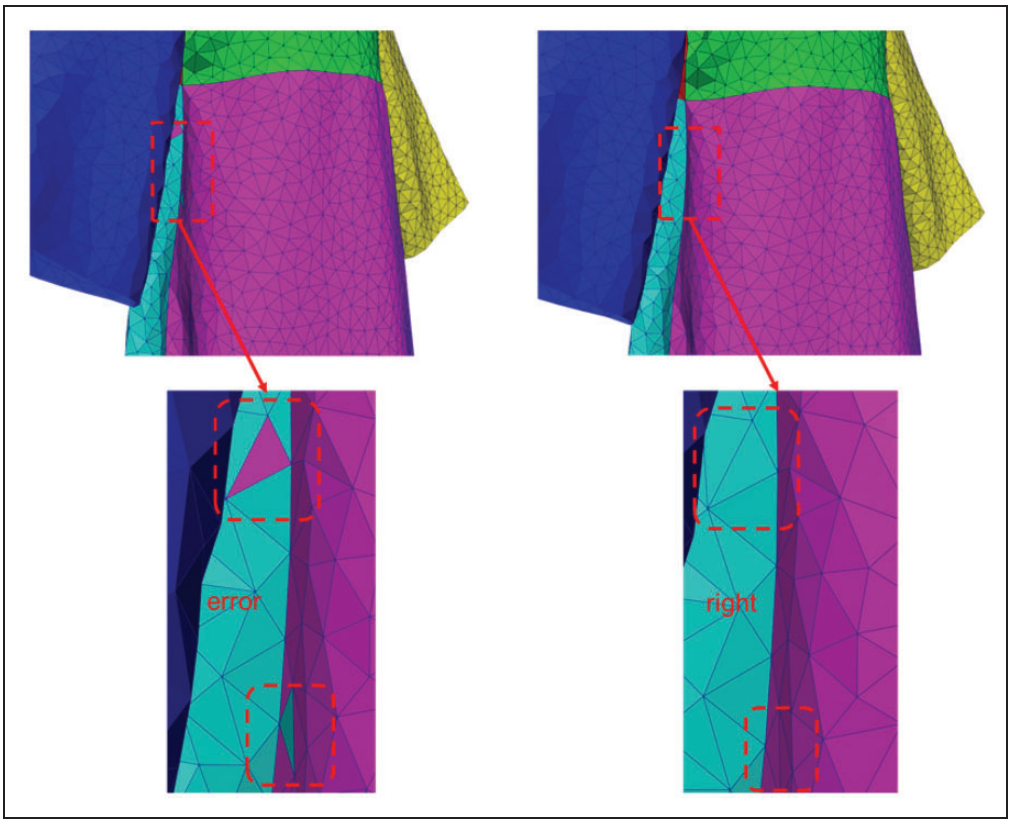

Figure 6. Compassion results of segmentation results without/with structural coherence loss on.

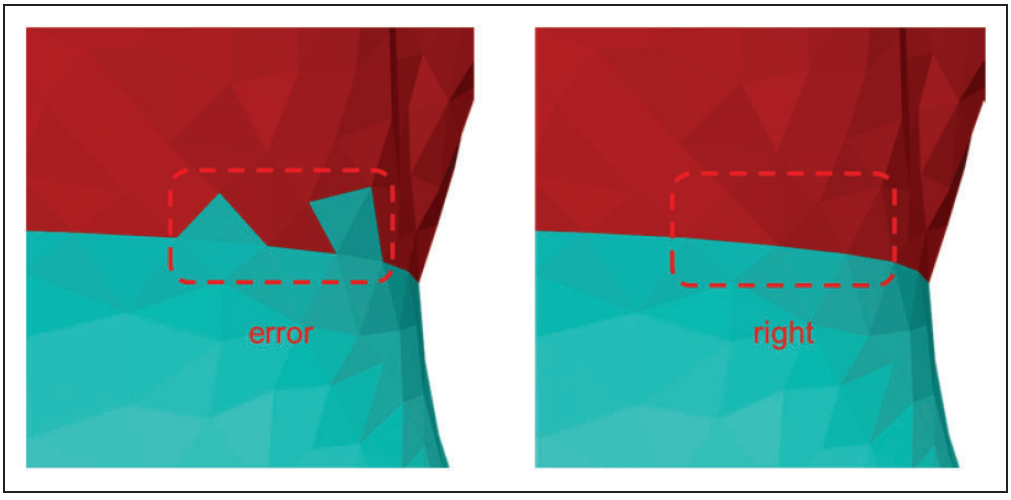

Figure 7. Result of segmentations before and after boundary optimization.

Table 2. Performance comparison of different module configurations

Model configuration	Average segmentation accuracy (%)	Training time (min)
Traditional graph transformer	99.96	35
Without dynamic attention fusion	99.98	24
Complete model	**99.99**	**23**

relies on traditional graph transformers, achieves a high accuracy rate of 99.96%. However, it comes at the cost of a 34% increase in training time. This highlights the significant advantage of the sparse attention mechanism, which effectively reduces computational complexity by selectively concentrating on essential node relationships, thereby streamlining attention computations.

Remarkably, the complete model attains optimal performance through the harmonious interplay of these two enhanced components. The global virtual node weighting module facilitates cross-regional feature correlations, whereas the sparse attention mechanism eliminates redundant computations through dynamic pruning. Together, they optimize both precision and efficiency, validating the soundness of the module design. These findings offer an interpretable and lightweight solution for the intricate task of 3D mesh processing.

Garment semantic segmentation results

To further evaluate the segmentation capabilities of the proposed model, this research undertakes a visual analysis of the segmentation results for four representative garment categories, as illustrated in Figure 8. The experimental findings reveal that the proposed sparse graph model effectively captures the geometric characteristics and semantic details of diverse garment components, producing distinct and coherent segmentation boundaries. For instance, in the segmentation of dresses, the model successfully distinguishes between elements such as the bodice, sleeves, and skirt hem. These results comprehensively affirm the robustness and generalizability of the proposed model in handling intricate garment structures.

To evaluate the generalization performance of the proposed model, this paper constructs a cross-domain test set for comparative experiments. The test set comprises 150 dress models from a public dataset,[29] with face counts ranging from 15,000 to 35,000, exhibiting significant distributional differences compared with the self-constructed dataset. A cross-validation approach is employed, incorporating 100 samples into the training process and designating the remaining 50 as an independent test set for performance assessment. After 27 minutes of training, the model completes inference for all test samples in 7.2 seconds, achieving an average segmentation accuracy of 99.91% (see Figure 9). This performance closely aligns with the 99.99% average accuracy obtained on the self-constructed dataset, with a minimal discrepancy of 0.08%. The consistent accuracy across diverse data distributions robustly confirms the model's adaptability to various garment pattern segmentation tasks. Specifically, the model sustains exceptional geometric segmentation precision for unseen dress models, thoroughly validating the robustness and generalization capabilities of the proposed algorithmic approach.

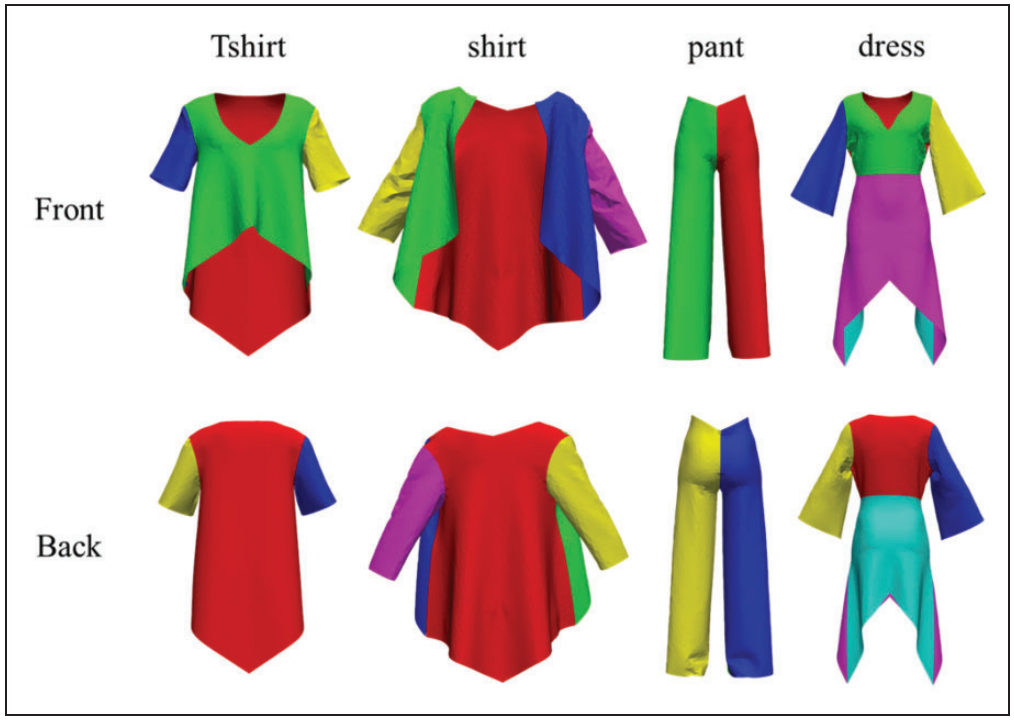

Figure 8. Comprehensive visualization of semantic segmentation performance on various garments.

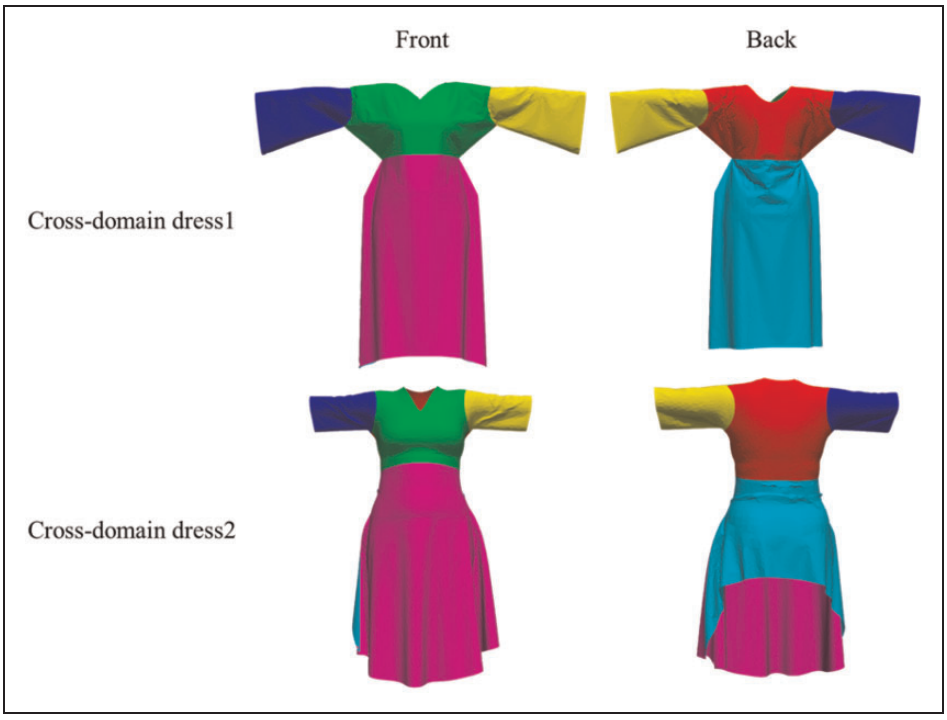

Figure 9. Cross-dataset generalization performance of the proposed semantic segmentation approach.

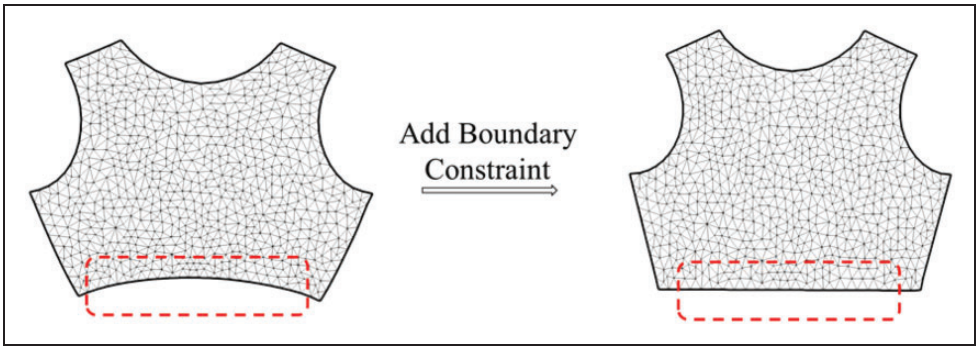

Figure 10. Boundary constraint effects on garment pattern geometry.

Effectiveness analysis of geometric constraints

Boundary constraints. Systematic experiments were conducted to evaluate the efficacy of the proposed boundary constraints in enhancing the geometric quality of 2D garment patterns. The effect of these constraints was assessed by comparing optimization outcomes with and without their constraints. The experiments utilized an example-based garment pattern model comprising both straight lines and spline curves. As depicted in Figure 10, in the absence of boundary constraints, optimized boundaries often exhibited irregularities, such as unevenness, unintended curvature, or distortions, particularly along edges intended to be straight. These deviations could compromise pattern-making accuracy and diminish product quality. In contrast, the application of boundary constraints resulted in smoother and more uniform boundaries, with straight lines preserved and curves refined into natural splines, aligning closely with engineering specifications.

Symmetry constraints. This section investigates the effectiveness of symmetry constraints in optimizing garment patterns and verifies their practical improvement through experiments.

An experiment was conducted using a pattern model with clear symmetric features. As shown in Figure 11, without symmetry constraints, the optimized pattern

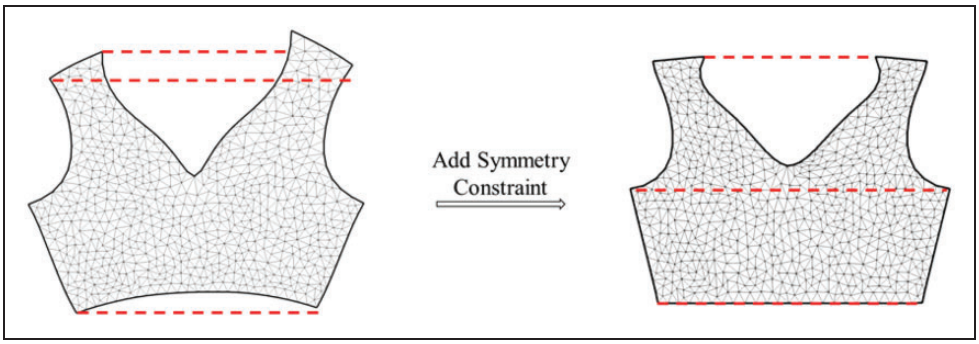

Figure 11. Symmetry constraint effects on single garment pattern geometry.

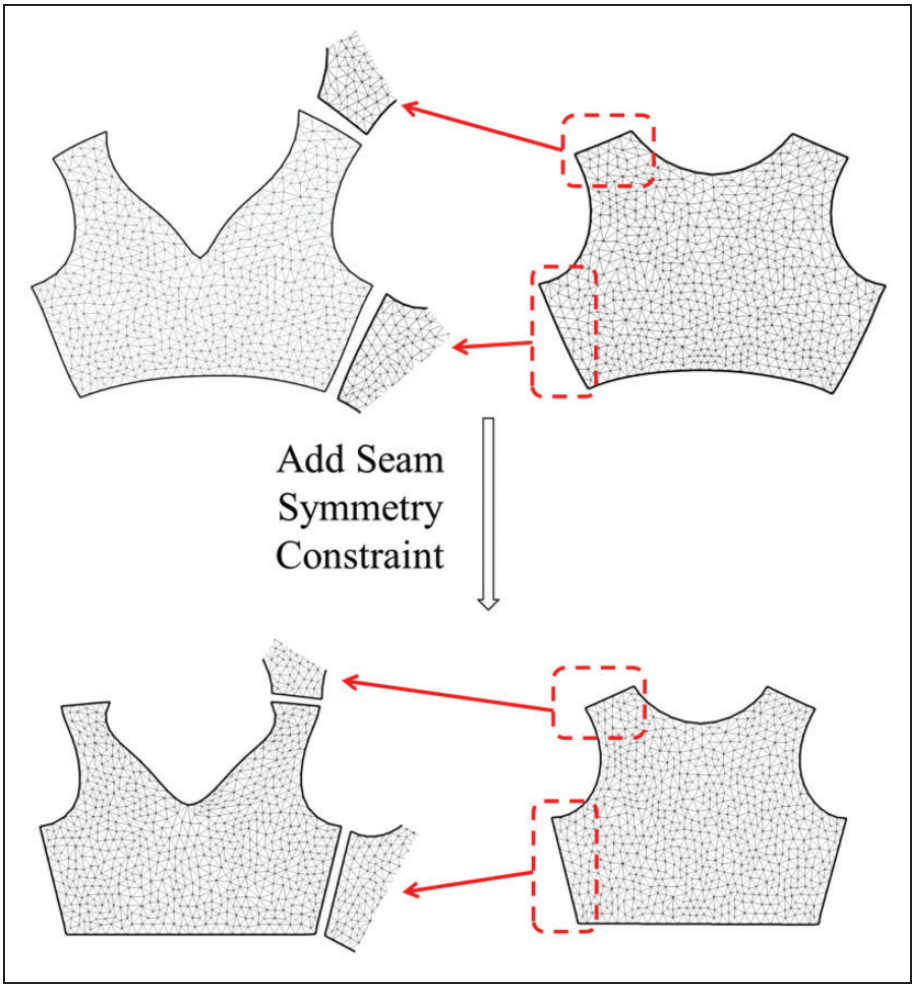

Figure 12. Reflective symmetry constraint effects on multigarment panel alignment.

could exhibit local distortions or asymmetric fluctuations, particularly in complex contour regions. These issues might increase processing complexity and reduce computational efficiency. With symmetry constraints applied, the pattern regained its intended symmetric structure.

Figure 12 further illustrates the effect of reflective symmetry constraints on indirect seams across multiple garment patterns. In the absence of these constraints, minor misalignments between corresponding boundaries could occur during parameterization. Although still sewable, these discrepancies might cause discomfort or wrinkles in the finished garment. With reflective symmetry constraints enforced, the boundaries exhibited greater consistency and symmetry, significantly

enhancing both aesthetic appeal and engineering usability, particularly for high-precision manufacturing applications.

Comparative experiments

Comparison of garment semantic segmentation results. To thoroughly assess model performance, Figure 13 presents a comparative analysis of experimental results between the sparse graph model proposed in this paper and two widely used segmentation methods across four categories of 3D mesh data: shirts, dresses, pants, and T-shirts. The conventional conditional random field method[20] exhibits an excessively protracted training duration of approximately 5 hours and produces higher boundary segmentation error rates. In contrast, the CAD-based BrepMFR method[8] achieves an average accuracy of 99.93% with a mean training time of 25 minutes. The proposed sparse graph model, which leverages hierarchical sparsification strategies, attains a superior average accuracy of 99.98% within a 23-minute training cycle. During testing, 50 garment patterns from each of the four categories were evaluated. The proposed model demonstrates a total processing time of 3.5 seconds, surpassing the BrepMFR method's processing time of 3.6 seconds, thereby highlighting the broad advantages of the introduced enhancement strategies.

The proposed method not only maintains an exceptional average accuracy of 99.98% but also demonstrates enhanced engineering applicability. As shown in Figure 14, the sparse graph model exhibits robust convergence from the outset of training, with an initial loss value of 0.3, approximately 40% lower than that of CAD-based methods. It achieves stable convergence in merely 20 iterations. Conversely, the loss curve of the BrepMFR model reveals persistent fluctuations over the first 50 iterations, indicating instability in parameter updates. These experimental results further

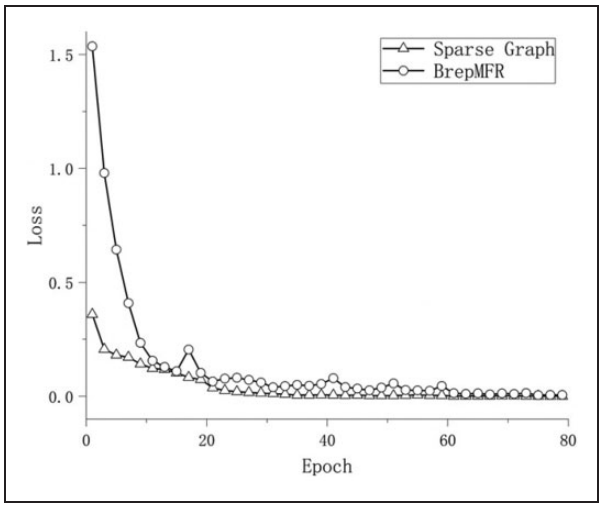

Figure 14. Loss values during the iterations for different methods.

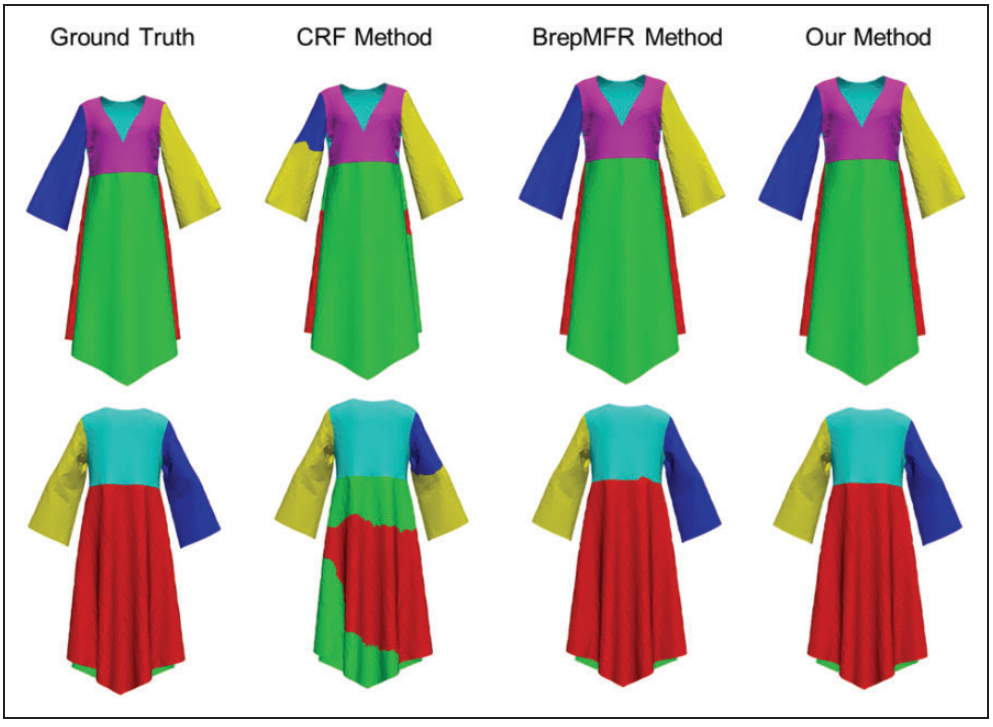

Figure 13. Comparative visualization of semantic segmentation performance among different models.

emphasize the significant benefits of the sparse graph model in terms of training efficiency and stability.

Comparison of garment pattern generation results from different methods. To further validate the training efficiency of the proposed model, systematic evaluations of the parametric properties of segmentation outcomes were conducted. Three comparative experimental groups were established, utilizing a self-constructed dataset (including dresses and T-shirts) and cross-domain datasets (incorporating third-party dresses), as illustrated in Figure 15. The proposed method was compared with the approach of Pietroni et al.[10] across multiple dimensions. Experimental results demonstrate that the garment panels generated by the proposed method exhibit superior structural rationality and boundary clarity. Across all test cases, the output consistently comprises either six or four regular panels, with symmetric edge features fully compliant with pattern-making specifications.

Comparative analysis reveals that the method of Pietroni et al.[10] generates a significantly higher number of panels under identical experimental conditions (38 panels for dresses, 14 for T-shirts, and 16 for cross-domain dresses), often accompanied by boundary distortions. Although this over-segmentation seeks to replicate fabric mechanical properties, it results in outputs that are challenging to integrate directly into production workflows. In contrast, the proposed method employs synergistic optimization of semantic understanding and parametric techniques to reduce the number of panels to standard production ranges,

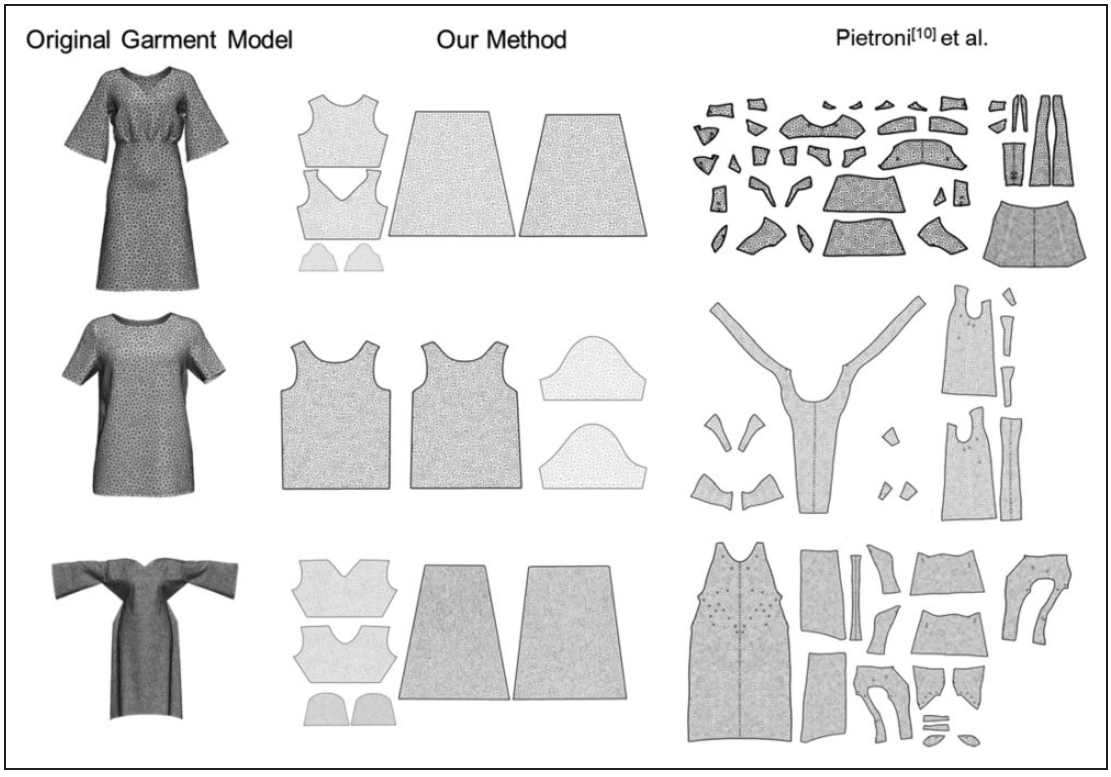

Figure 15. Pattern generation results of different models.

Table 3. Comparative analysis of the efficiency of different version generation methods

Garment type	Number of faces	Method	Generated panels	Patch generation time (s)	Parameterization time (s)	Structural consistency (%)
dress	10,948	Our method	6	1.5	17	100
		Pietroni et al.	38	91	18	5.13
T-shirt	10,364	Our method	4	1.4	17	100
		Pietroni et al.	14	74	17	8.74
Cross-domain dress	28,026	Our method	6	3.2	43	100
		Pietroni et al.	16	138	43	10.56

while maintaining geometric precision and ensuring smooth, symmetric characteristics across all panel boundaries.

Quantitative data in Table 3 highlight the comprehensive advantages of the proposed method. In terms of segmentation efficiency, standard dress cases require only 1.5 seconds, achieving a 60× acceleration compared with traditional methods. For complex cross-domain models with 28,026 face patches, segmentation time is maintained at 3.2 seconds, reflecting a 43× improvement over comparative methods, while parametric time consumption remains comparable to conventional approaches. The proposed pattern generation method fully considers practical pattern-making specifications, facilitating seamless integration into garment production workflows. Consequently, the model demonstrates significant enhancements in the practicality and operability of generated garment patterns.

In terms of structural consistency of garment patterns, experimental results show that for different types of garments such as dresses and T-shirts, the method in this paper achieved 100% similarity, significantly better than the 5.13% and 8.74% reported by comparison methods. In addition, on dress models from a public dataset, this paper's method also reached 100% similarity, much higher than the best previously reported result of 10.56%. This shows that the proposed method has significant advantages in accuracy and robustness, making it suitable for analyzing garment models with complex structures.

To ensure a more rigorous and unbiased comparison of fabric stretching during the parametric flattening process, this study applies the proposed flattening optimization method and the comparative method developed by Pietroni et al.[10] to the same garment semantic segmentation results. As detailed in Table 4, across three representative garment types, dresses, T-shirts, and cross-domain dresses, the proposed method records stretch measurements of 0.03, 0.0157, and 0.0378, respectively, whereas the comparative method yields values of 0.0112, 0.0126, and 0.0189 for the corresponding categories. Although the comparative method exhibits slightly lower stretch values, suggesting a minor advantage in local stretch control, the proposed method demonstrates superior performance in boundary formation. By generating more regular and smooth boundaries while preserving the number of garment panels, it significantly improves sewing efficiency. This advantage is further illustrated in Figure 16, which presents a direct visual comparison of the flattening outcomes of both methods on an identical dress model. The upper row, showcasing the results of the proposed method, starkly contrasts with the lower row depicting the comparative approach. Despite its favorable local stretch values, the comparative method, lacking explicit boundary constraints, produces distorted and irregular boundaries. This not only compromises the visual integrity of the flattened patterns but also reduces their practical utility in real-world applications.

Table 4. Comparison of stretching metric *D* across methods

Method	Dress	T-shirt	Cross-domain dress
Our method	0.03	0.0157	0.0378
Pietroni et al.	0.0112	0.0126	0.0189

Evaluation of generated patterns by virtual stitching

To verify the industrial feasibility of the garment patterns generated in this paper, a virtual stitching experiment was conducted. The boundaries of all the generated patterns were extracted and saved as DXF files, which were subsequently imported into Style3D software. Within this software environment, virtual stitching and physical simulations were executed to reconstruct virtual garment models. These reconstructed models were then compared with the original 3D garment models. As illustrated in Figure 17, the two sets of reconstructed garments demonstrated a high degree of congruence in overall shape, with only negligible discrepancies in local details. The

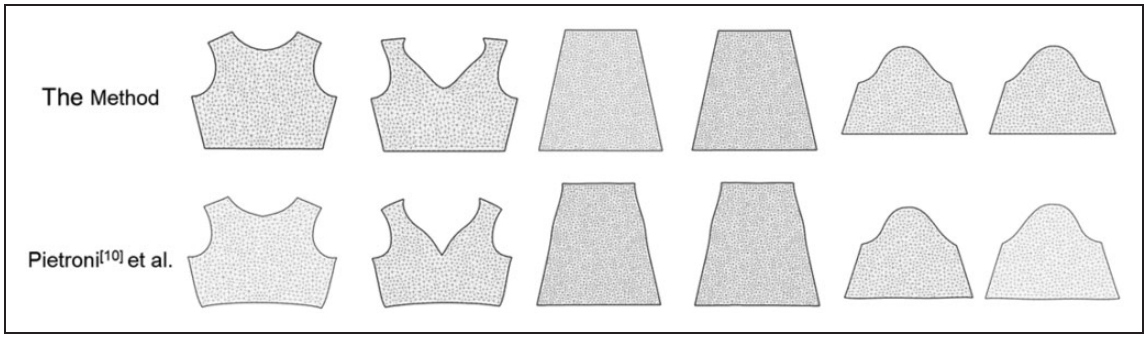

Figure 16. Comparison of flattening results under the same segmented panels.

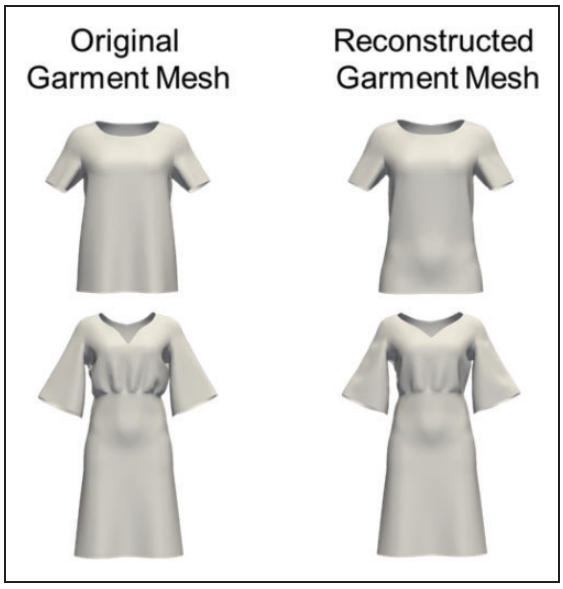

Figure 17. Comparison between the original garment mesh and the reconstructed garment mesh.

experimental results strongly suggest that the generated patterns exhibit excellent sewability and structural soundness, thereby fulfilling the requirements of digital garment design.

Conclusions

In this paper we have proposed an example-based method for automatic garment pattern generation, integrating semantic segmentation using sparse GNNs with boundary and symmetry optimization strategies. We have effectively addressed the key challenge of balancing efficiency and accuracy in digital pattern design. Experimental results show that the method achieves a segmentation accuracy of 99.99% on 3D mesh data, and maintains a high accuracy of 99.91% on cross-category models, significantly outperforming current state-of-the-art approaches. Furthermore, thanks to the lightweight design of the sparse graph transformer, the training time is reduced by 34%.

In terms of output quality, the proposed method achieves 100% structural similarity with template patterns for dresses and T-shirts. The generated patterns exhibit smooth edges and well-organized layouts that fully comply with industrial grading standards. Although the stretching ratio (0.0157–0.0378) is slightly higher than that of baseline methods (0.0112–0.0189), the resulting geometric regularity and manufacturability significantly reduce cutting errors and enhance overall production stability and reliability.

However, our method relies on predefined templates, limiting its generalization capability for asymmetric or highly stylized garments such as avant-garde fashion pieces. Future work will focus on enhancing the system's adaptability through data-driven approaches based on deep learning models, including autoencoders, style transfer networks, and self-supervised feature extractors. The goal is to enable template-free pattern generation by learning from large-scale 3D clothing datasets, allowing the system to automatically construct suitable base structures based on input characteristics such as silhouette, drape, and functional constraints. This advancement will significantly improve the system's flexibility and applicability in both creative and industrial contexts.

Data availability

The primary dataset used in this study is a self-constructed collection developed specifically for this research. While our experimental implementations reference the ETH Zurich dataset[35] for comparative analysis and methodology validation, the core data analyses are based on our proprietary dataset. For transparency regarding the referenced external data, the ETH Zurich dataset is publicly available under the repository's license terms at: https://www.research-collection.ethz.ch/handle/20.500.11850/673889

Declaration of conflicting interests

The author(s) declared no potential conflicts of interest with respect to the research, authorship, and/or publication of this article.

Funding

The author(s) disclosed receipt of the following financial support for the research, authorship, and/or publication of this article: This work was supported by the Key R&D Programs of Zhejiang Province (grant number 2024SJCZX0026).

ORCID iDs

Roujia Hong https://orcid.org/0009-0006-8164-3930
Yarui Zhang https://orcid.org/0009-0003-7924-8358
Yao Jin https://orcid.org/0000-0001-9518-7063

References

1. Srivastava A, Manu P, Raj A, et al. WordRobe: Text-guided generation of textured 3D garments. In: *European Conference on Computer Vision*. Cham: Springer Nature Switzerland, 2024, pp. 458–475.
2. Umetani N, Kaufman D, Igarashi T, et al. Sensitive couture for interactive garment modeling and editing. *ACM Trans Graph* 2011; 30(4): 90.
3. He K, Yao K, Zhang Q, et al. DressCode: Autoregressively sewing and generating garments from text guidance. *ACM Trans Graph* 2024; 43(4): 72.
4. Zhou Y, Jiang H, and Chen L. Automatic pattern-making of Chinese wedding dress based on AutoCAD parameterization. *J Text Sci* 2022; 43(9): 175–181 (in Chinese).

5. Chen X, Zhou B, Lu F, et al. Garment modeling with a depth camera. *ACM Trans Graph* 2015; 34(6): 203.
6. Korosteleva M and Lee S. Neuraltailor: Reconstructing sewing pattern structures from 3D point clouds of garments. *ACM Trans Graph* 2022; 41(4): 158.
7. Bang S, Korosteleva M, and Lee S H. Estimating garment patterns from static scan data. *Comput Graph Forum* 2021; 40(6): 273–287.
8. Zhang S, Guan Z, Jiang H, et al. BrepMFR: Enhancing machining feature recognition in B-rep models through deep learning and domain adaptation. *Comput Aided Geomet Des* 2024; 111: 102318.
9. Shirzad H, Velingker A, Venkatachalam B, et al. Exphormer: Sparse transformers for graphs. In: *International Conference on Machine Learning*. PMLR, 2023, pp. 31613-31632.
10. Pietroni N, Dumery C, Falque R, et al. Computational pattern making from 3D garment models. *ACM Trans Graph* 2022; 41(4): 157.
11. Wang Z, Xing Y, Wang J, et al. A knowledge-supported approach for garment pattern design using fuzzy logic and artificial neural networks. *Multimedia Tools Applicat* 2022; 81: 19013–19033.
12. Jin P, Fan J, Zheng R, et al. Design and research of automatic garment-pattern-generation system based on parameterized design. *Sustainability* 2023; 15(2): 1268.
13. Korosteleva M and Sorkine-Hornung O. GarmentCode: Programming parametric sewing patterns. *ACM Trans Graph* 2023; 42(6): 199.
14. Yang S, Pan Z, Amert T, et al. Physics-inspired garment recovery from a single-view image. *ACM Trans Graph* 2018; 37(5): 170.
15. Gou B, Cai C, Kang Q, et al. Garment pattern recognition method based on artificial Intelligence algorithm. In: *2022 5th World Conference on Mechanical Engineering and Intelligent Manufacturing*. IEEE, 2022, pp. 1076–1079.
16. Liu L, Xu X, Lin Z, et al. Towards garment sewing pattern reconstruction from a single image. *ACM Trans Graph* 2023; 42(6): 200.
17. Chen C, Su J, Hu M, et al. Panelformer: Sewing pattern reconstruction from 2D garment images. In: *Proceedings of the IEEE/CVF Winter Conference on Applications of Computer Vision*, 2024, pp. 454–463.
18. Huang X, Hou Y, Yang Y, et al. Automatic generation of high-precision garment patterns based on improved deep learning model. *J Text Sci* 2025; 46(2): 236–243 (in Chinese).
19. Xiao B, Shi J, Wang Y, et al. Personal pattern generating method for speed skating suits. *J Beijing Inst Fash Technol* 2023; 43(2): 64–70 + 84 (in Chinese).
20. Kalogerakis E, Hertzmann A, and Singh K. Learning 3D mesh segmentation and labeling. In: *ACM SIGGRAPH 2010 Papers*. New York: ACM Press, 2010, pp. 1–12.
21. Schneider R and Tuytelaars T. Example-based sketch segmentation and labeling using CRFs. *ACM Trans Graph* 2016; 35(5): 151.
22. Liu L, Wang R, Zhou F, et al. Semantic segmentation and labeling of 3D garments. In: *2014 5th International Conference on Digital Home*. Piscataway, NJ: IEEE, 2014, pp. 299–304.
23. Guo K, Zou D, and Chen X. 3D mesh labeling via deep convolutional neural networks. *ACM Trans Graph* 2015; 35(1): 3.
24. Xu X, Liu C, and Zheng Y. 3D tooth segmentation and labeling using deep convolutional neural networks. *IEEE Trans Visualiz Comput Graphi* 2018; 25(7): 2336–2348.
25. Li J and Lu G. Modeling 3D garments by examples. *Computer-Aided Des* 2014; 49: 28–41.
26. Boykov Y, Veksler O, and Zabih R. Fast approximate energy minimization via graph cuts. *IEEE Trans Pattern Anal Machine Intell* 2002; 23(11): 1222–1239.
27. Wolff K, Herholz P, and Sorkine-Hornung O. Reflection symmetry in textured sewing patterns. In: *Eurographics Proceedings of Vision, Modeling and Visualization*, 2019, pp. 11–18.
28. Gal R and Cohen-Or D. Salient geometric features for partial shape matching and similarity. *ACM Trans Graph* 2006; 25(1): 130–150.
29. Korosteleva M, Kesdogan TL, Kemper F, et al. GarmentCodeData: A dataset of 3D made-to-measure garments with sewing patterns. In: *European Conference on Computer Vision*. Cham: Springer Nature Switzerland, 2024, pp. 110–127.